Supplement of Atmos. Meas. Tech., 7, 3611–3621, 2014
http://www.atmos-meas-tech.net/7/3611/2014/
doi:10.5194/amt-7-3611-2014-supplement

Atmospheric Measurement Techniques Open Access

Supplement of

Amine permeation sources characterized with acid neutralization and sensitivities of an amine mass spectrometer

N. A. Freshour et al.

Correspondence to: D. R. Hanson (hansondr@augsburg.edu)

24 pages, 22 figures.

Summary.

A description of AmPMS sampling arrangement and how the background signals were obtained in the field studies are described in the first two sections (S1.1 and S1.2). Tests of an acid scrubbing tube and a comparison to the catalytic converter method for removing bases from the sample are described in section 1.3. Response times due to surface interactions of amines with surfaces are discussed next (sections 1.4-1.5). Detection limits and the interpolation scheme used between background determination are discussed in 1.6 and 1.7. Low reagent ion count rate episodes in the field studies are discussed in 1.8 and the ambient data for the rest of the Lewes and Oklahoma campaigns are shown in 1.9. Comments regarding the AmPMS data sets including Atlanta, 2009 are given in 1.10. Calibration for DMSO is discussed in section 2 and measurements of other species by AmPMS in Lewes, DE are presented in section 3. Section 4 presents diurnal averages from the Oklahoma campaign and section 5 shows correlation plots from the Lewes study.

Addition of amines to a nucleation flow reactor are described in section 6 along with CFD simulations of the dispersal of the amine into the main flow within the reactor.

Lastly, a tandem titration experiment is presented and the time and temperature dependencies of the permeation rate of select permeation tubes is presented in section 7.

SI 1.1 AmPMS ambient sampling and inlet lines.

As deployed in the field, AmPMS samples air (~1200 sccm) through an inlet of ~4.5 mm ID tube that is ~ 3 to 5 m in length to sample air a few m from the building. Just before the ionization region, the sample gas passes through a Teflon union adaptor (1/4" to 3/8") then through a Teflon tee and into the glass manifold of the instrument that surrounds the ionization source, the drift region and the mass spectrometer inlet. The tee allows for supplanting the sample gas flow with a flow of catalytically cleaned air to determine instrument background signals (the "zero" procedure). Sample air flows straight through the tee while clean air during a zero makes a right turn (Fig. S1A).

The catalytic converter (AmPMS) provides clean air for determining the instrument background levels and also for the ion source, about 40 sccm. This air flows over a vial that contains a dilute HNO_3 aqueous solution (initial HNO_3 concentration of about 5 wt %) that provides water and HNO_3 vapor for the ion source (four 0.9 µCi Am-241 tabs). The acid vapor (about 1 ppmv) helps suppress ammonia and amine background signals believed to originate in the source. A mass spectrum of ambient air is shown in Fig. S1B.

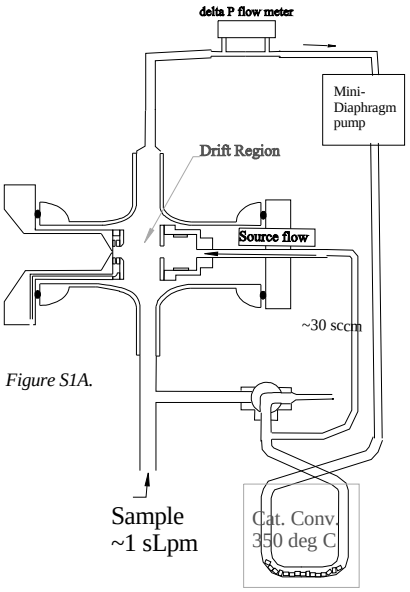

Figure S1A.

Fig. S1B. Mass spectra from AmPMS deployment in Oklahoma, early in the campaign, 2013Apr16. Top scale (kHz) shows reagent ions NH_4^+, $H_3O^+\cdot(H_2O)_{1,2}$ as the majority ions. Bottom scale is finer and shows signals for the alkyl amines (plus BG signals) and other ions, some of which are discussed in the following sections.

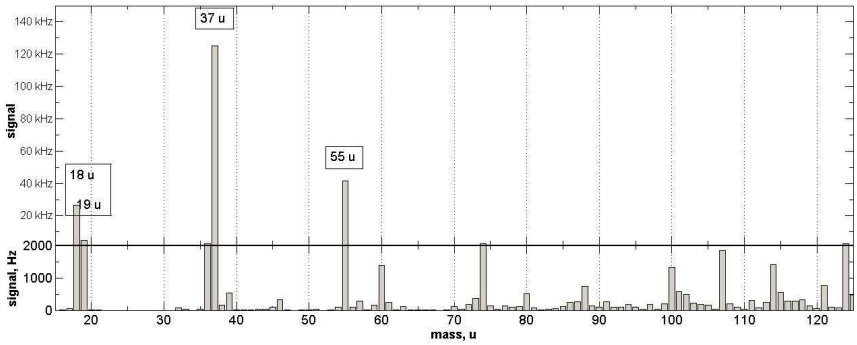

The mass spectra shows that the reagent ion clusters, $H_3O^+\cdot(H_2O)_{5,6}$, are stripped of most of their water ligands. The majority of the non-reagent masses with significant count rates are attributable to amino species and they are also stripped of water ligands.

The sample gas flow (1200 sccm) and source flow rates are monitored with delta P laminar flow meters (tubes of ~1/16" and 1/32" inner diameter, respectively) where the pressure drops are about 1 and 0.5 kPa, respectively. During sampling of outdoor air through ~5 m of 1/4" OD tubing, the drift region pressure is about 0.2 kPa below ambient pressure. Pressure sensors are piezo type (MPXV7002 or 5004, Freescale semiconductor, see note 1). The mini-diaphragm pump (HiBlow USA, CD-8-1101) has a free air flow rate of ~13 L/min which is throttled down to 1200 sccm by the catalytic converter and a small tube on the outlet of a three way solenoid valve. This valve is normally set to vent to ambient through this small tube and the size of the tubing is determined such that the source flow rate does not change when the valve is actuated and clean air is sent to recycle through the drift region.

Background signals are determined by actuating the valve which initiates a 'zero' where the sample air is replaced by catalytically cleaned air of the same relative humidity. Maintaining a constant relative humidity minimizes changes in background signals. Background signals are also dependent on the temperature of the drift region (monitored with a LM35DZ.) Typical zero time period is 15-20 min and a zero is initiated every 1 to 2 hr.

The curtain gas *(Hanson et al. 2011)* has not been used for the past two field deployments (July 2012 in Lewes DE and Apr 2013, Lamont, OK.) Using a curtain gas without precise humidity control would significantly affect signals during the zeroing procedure (see note 2). The instrument also does not require pressurized gas cylinders. The disadvantage is the exposure of the orifice to large dust particles or fibers in ambient air. A clog in or near the orifice has happened the past two deployments evidenced by the pressure on the vacuum system decreasing by 20 to 50 % and ion count rates decreasing by 50 to 90 %. Visual verification of the clogs using a microscope was done after the measurement campaigns. See SI1.8 for discussion on how the measurements were affected

A new procedure and flow setup that incorporates a second catalytic convertor and pump for introducing curtain gas is planned for future deployments. This would address a potential small bias (≤10%) and diminish the occurrence of ion orifice clogs.

SI 1.2 Zeroing behavior: BG determination.

SI 1.2.1 Regular BG determination

Reliable AmPMS data requires the determination of instrument background signals periodically. This was done every 1 or 2 hours by supplanting most of sample gas with recirculating clean gas of the same RH. Temperature, RH, and time all affect the background signal (BG) for most species and extracting abundances for species with large BG are especially vulnerable to its fluctuations. Artifact swings in concentrations can be introduced by quick (~ 1 hr) and large changes in temperature or RH.

The temporal behavior of the amine signals indicated interactions with surfaces. Over time, surfaces in the ion drift region can accumulate material (most likely dust or aerosol particles) and there is evidence that degassing of amines from these surfaces can contribute to the observed signals and cause the instrument response to be sluggish. For example, after the first two weeks of the field campaign in Atlanta *(Hanson et al. 2011)*, the ammonia signal became unusable for deriving ammonia abundances, due to an increased BG level as well as lower NH_3 abundances. BG for NH_3 was not successfully determined at these times; even negative net abundances (false negatives) could be inferred from the data. In the recent Lamont OK campaign this sluggishness was also observed for ammonia and most of the amines. At times swings in abundances resulted in negative values due to inaccurate BGs. The instrument when it was deployed in Lewes DE did not suffer nearly as much from these sluggish intervals.

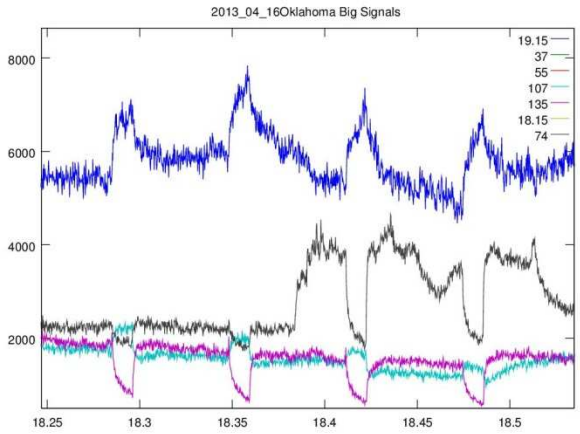

Figure S2. Time sequence showing zero-ing behavior. Raw signals in Hz plotted versus time in days. The signals at 37 and 55 u are off scale.

Normal behavior of AmPMS background determination is depicted in Fig. S2, a plot of signals (Hz at masses: 19.15 u 74 u, 107 u, 135 u) vs. UT day for 2013Apr18. Zeroes are easily seen in the C4-amine data (74 u) and the 135 u data, which is likely a VOC with a high proton affinity, e.g. tetramethyl benzene. The species detected at 107 u is believed to be related to the pressure sensor that monitors the source flow (see note 1). Upon a zero and upon sampling again, the signals rise quickly while during each zero (about every 2 hrs) the 74 u and 135 u BGs steadily decrease. Signal for one of the reagent ions, 19 u, shows behavior common to all the reagent ions upon a catalytic converter (CC) zero. Any changes in the water proton cluster signals that occur during a zero are taken into account in the extracted mixing ratio. The normal procedure for most time periods and most masses is to retain the last third of the zero data as BG. In addition, the first ~10 minutes of sample data after each BG is

discarded. The mixing ratio for the C4 amine, 74 u, shows good behavior in this sense during this time period. A large increase in this amine occurs at 18.38 d. In addition, see Figs. S4a,b for data that shows signals exhibiting typical behavior during a series of zeroes.

SI 1.2.2 Possible source of BG ions.

One of the comments from referee 3 concerning the relative humidity dependence of AmPMS' BG levels stimulated much consideration on the source of the BG signals. Previous work on the NH_3 BG signal within AmPMS' predecessor found that it was proportional to water vapor and concluded that it was due to processes within the ion source (*S35*). With this backdrop, we consider here that a significant source for the BG ions is within the ion source, perhaps from surfaces that are close to the ambient sample air. This is supported by two observations: (1) that the BG signal levels for many of the amines were somewhat correlated to the previous history of that particular amine in the sample air and (2) that there is a significant RH dependence. Back diffusion into the ion source cavity could explain in part observation (1) and perhaps (2). The strong RH dependence (2) can be due in part to small changes in conditions within the source due to the RH variations in the source flow which is primarily determined by ambient water vapor.

A rough comparison of the source flow rate and a crude deposition velocity shows that diffusion of ambient species into the ion source can be significant: (i) with a source flow of ~ 30 sccm, the average flow velocity through the ion exit hole (0.6 cm diameter) is 1.7 cm/s and (ii) a rough deposition velocity is ~1.2 cm/s (estimated from the ratio of the diffusion coefficient, ~0.1 cm^2/s, to the thickness of the exit plate). This crude comparison suggests that back diffusion needs to be investigated experimentally.

The water content of the source flow is largely set by the ambient RH because the vial teed into the source line was not designed to fully humidify this flow. The vial works by diffusion of water vapor (and HNO_3 vapor) which requires a concentration gradient and therefore cannot provide steady RH conditions when there are changes in RH at the top of the diffusion tube. Since the residence time of ions in the source can be relatively long due to weak electric fields within it, even very small amounts of amines that are influenced by RH in the source can lead to significant signal levels that are RH dependent. These small levels can take a very long time to flush out of the source and thus the BG levels can stay elevated for hours to days after exposure to a relatively high level of amines or ammonia.

To better detect low levels of amines, the BG signals of AmPMS should be minimized. When AmPMS becomes operational again, changes to its setup will be investigated. For example, a source flow arrangement with a constant RH will be tested and changes to the dimensions of the ion exit hole and dependencies on the total flow through the source will be explored.

SI 1.2.3 Sluggish zeroes.

In contrast to the normal zeroing behavior discussed in SI1.2.1 above, at times abnormal behavior in BG levels for the amines was observed. It is thought that material can accumulate on surfaces within the ion drift region or in the tee just preceding it, which can adversely affect the CC zeroing mechanism. Also, there were occasional 'clogs' in the ion sampling orifice: at times there was a severe depletion of reagent ion signals (depletion > 90 %; see SI1.8 below.) Nonetheless, an alternate procedure for determining BGs was developed.

Sluggish behavior in the BGs for dimethyl amine (46 u) is illustrated in Fig. S3. Dimethyl amine generally had a large BG to signal ratio, with BG mixing ratios equivalent to several hundred pptv at times. Also, the C4-amine at mass 74 u had BG equivalent to a few ppbv at times. Signals are converted to pptv in Fig. S3. Mixing ratios typically decrease upon a zero but during sluggish periods the data, e.g. for 46 u in the figure, initially shows an increase (zero starts at: 21.75 21.83, 21.92) and then falls slowly over the next 20 to 30 min. Furthermore, when the CC zero was stopped, the data did not begin to rise

until 20 or 30 min had elapsed. This sluggish behavior has a significant effect on determining the net mixing ratio for those compounds with large BG to signal ratios. Signals for mass 59 and 121 are likely due to VOCs (acetone etc.) and their relative abundance are shown in Fig. S3 as they respond well to CC zeroes.

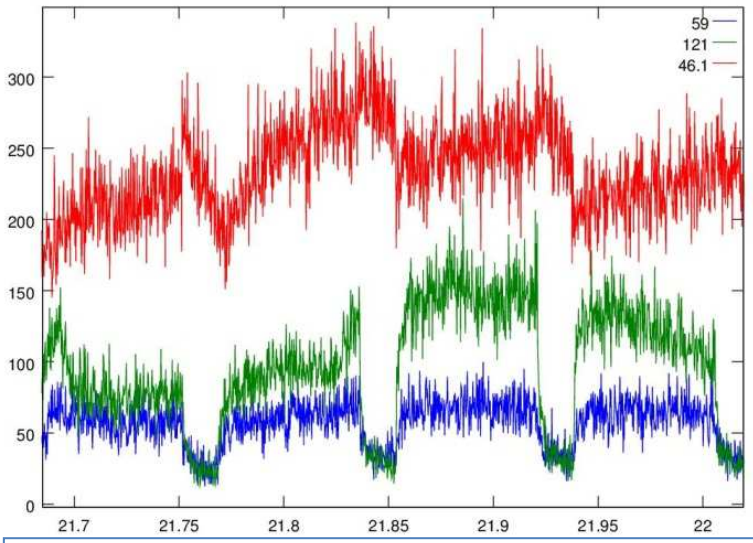

Fig. S3. Mixing ratio for dimethyl amine (46.1) in pptv, and relative mixing ratios for VOCs acetone (59) and C9 aromatic (121) plotted versus time in days. Signals for VOCs were converted to pptv using S_{typ} and actual ambient mixing ratios in pptv are several hundred times these values.) Zeroes for the VOCs are distinct and background signals are well-monitored while the dimethyl amine backgrounds are not.

The alternate BG determination is to postulate that a 'delayed' zero occurs. Data for the ten minutes after the zero was stopped was used as the BG level. So instead of discarding the first ~10 min of data after a zero is initiated, this data is used as the zero and the CC zero data is discarded. Thus, the first ten minutes of data after a CC zero that is usually discarded is instead used as BG. Whether to use the normal procedure or the sluggish procedure was determined by taking the greater of the resulting mixing ratios.

Methyl and dimethyl amine mixing ratios were most affected by the sluggish behavior because of their generally low levels and relatively high BGs. Over 80% of the data for these compounds during the Oklahoma campaign was analyzed using the sluggish procedure. 70 % of the ammonia data were sluggish, while 50 % of 60 u, 74 u, 102 and 116 u amines mixing ratios were generated using the sluggish procedure. The data for the C5 amine detected at 88 u was less than 1 % sluggish due to a generally high ambient level compared to its BG level.

SI 1.2.4 Bias in ambient amines due to sluggishness.

The delayed zero procedure only partially takes into account the stickiness of the amines: for many periods of time the data for ammonia and dimethyl amine show a rise over the ~1.5 hr time between zeroes. During these times, the abundances of these species are probably biased low because zeroes were probably biased slightly high. Also, for most time periods when sluggishness was displayed, the data for the affected masses showed a rise to an asymptote, apparently when amine levels were stable on the hour-long time scale. The best data for these time periods and these masses are the 45 min of data just before a zero is initiated. As the data shows that the first 45 min is low (as much as 30 %) from the later data, the two hour averages are biased slightly lower than the actual 2 hr abundances.

As discussed below (SI1.4-5), sticking of the methyl amine and ammonia in the ~ 4 m inlet is also significant, although the larger amines appear to have much smaller interactions with the inlet surfaces. Evidence is presented that the full amount of amine eventually travels down the inlet so that in principle no bias is introduced. However, the temporal evolution of ambient amines is smoothed out and delayed by the inlet. This time delay is estimated to be up to an hour for methyl amine (for an inlet used for many weeks) but for trimethyl amine this delay is less than a minute for capturing 50 % of a rapid change and perhaps ten minutes for capturing the full change.

SI 1.2.5 Possible causes of Sluggishness

We propose that the sluggish behavior of the zero determination discussed in 1.2.3 is primarily due to reasons other than that discussed above for the overall BG levels and their RH dependence (see

1.2.2). This is supported by the fact that the sluggish behavior was not exhibited in all the campaigns: it was primarily seen in the data for the Oklahoma campaign.

Possible causes for sluggishness include: (i) The presence of semi-volatile carboxylic acids: the zero removes all species, bases and acids, thus the surfaces in the ionization region can release base that had been tied up by acid, causing an increase in the AmPMS signal for some amines. Once the sample flow is re-established, the acid once again suppresses base evaporation from surfaces, and this is more representative of baseline conditions for the instrument, until gas-phase amine reconditions surfaces leading to the ionization region. (ii) Aerosol material that had deposited in the tee during sampling. This tee is where catalytic converter air enters AmPMS during a zero and aerosol material could emit amines during a catalytic converter zero. (iii) If material is deposited inside AmPMS drift region especially on the ion inlet orifice disk. If this material is next to or slightly occluding the orifice, then reagent ions can interact with this material. (iv) Material could accumulate near or in the ion source. Both (iii) and (iv) might cause a jump in BG signal during a catalytic zero because the reagent ion signals increase during the catalytic zero (partly due to removal of reacting species but also partly due to the small pressure change). (v) Ammonia and amine vapor that deposited on the non-smooth transitions in the sampling tee or the fitting between the glass and tee. During a zero, the flow changes from straight through to making a right angle, and this disturbed flow may entrain this deposited material. (vi) Adhesion of amines to surfaces in the curtain region, which was not flushed with curtain gas in either the Lewes or the Oklahoma campaigns.

Changes to AmPMS protocol to understand this sluggishness will be explored. Changes to the geometry of the tee where the catalytic convertor air supplants the ambient air and how this may affect the zero determination will be explored. The curtain gas will be reinstated in future AmPMS deployments which will help repel orifice-clogging material (see SI1.8) from the curtain region and also might eliminate some sluggishness in the BG determination, item (vi) above.

SI 1.3 Amine Scrubbing with acid-doped tubing.

An alternative to CC zero-ing for determining the background signals was used for outdoor air sampled in November, 2013 in Minneapolis. Two acid scrubber tubes (i.e., denuders) were prepared with ¼" OD Teflon tubes: a 30 cm length of tubing was immersed in 6 M H_2SO_4 solution for several minutes, and a 70 cm length of tubing was immersed in a 20 % phosphoric acid solution. The tubes were allowed to dry after the immersion (no rinsing) in a clean flow of nitrogen, and they were used to obtain BGs for the alkyl amines. In between CC zeroes, the sulfuric acid tube was manually placed in line with the sample gas for a period of time. The results of a series of 30 cm acid scrubber experiments showed that zero levels for ammonia and amines were similar to the CC zero with perhaps the exception of the heavier amines, from 88 to 116 u. One such scrubber test is shown in Fig. S4a. The heavier amines may not have been removed as efficiently by the scrubber due to slower diffusion to the scrubber wall.

To test the acid scrubber over long periods of time, the three way valve was put just before the AmPMS inlet (as AmPMS was deployed in Atlanta 2009 Hanson et al. 2011), and a zero was measured by diverting the sample gas through a scrubber before entering the drift region. A subset of this data is shown in Fig. S4b which depicts five minute-averaged mixing ratios versus time (day in Nov.) with the zeroes clearly distinguished.

Fig. S4a. Amine mixing ratios (pptv) vs. fractional day for AmPMS sampling urban air (Minneapolis, MN, 2013Nov04.) Zero levels have not been subtracted from the data. The regular (2.03 hr = 0.085 d interval) catalytic zero and the scrubber zero at 4.79 d are in good agreement. The ammonia signal behaved similarly. Net amine signals range from a few pptv to a few tens of pptv (methyl amine, 32 u: blue; dimethyl amine, 46 u: green; TMA, 60 u: red; C4-amine, 74 u: aqua; 88u: magenta; 102 u: gold; 116 u: black.)

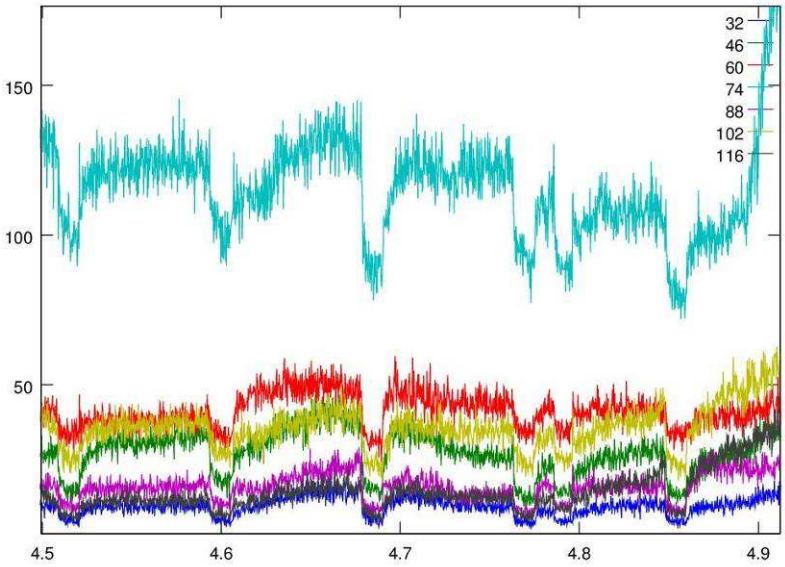

Fig. S4b. Net amines using Acid Scrubbing Tube for zeroes with 5 min data for C1, C2 and C3 amines. Outdoor air in Minneapolis, Nov 2013.

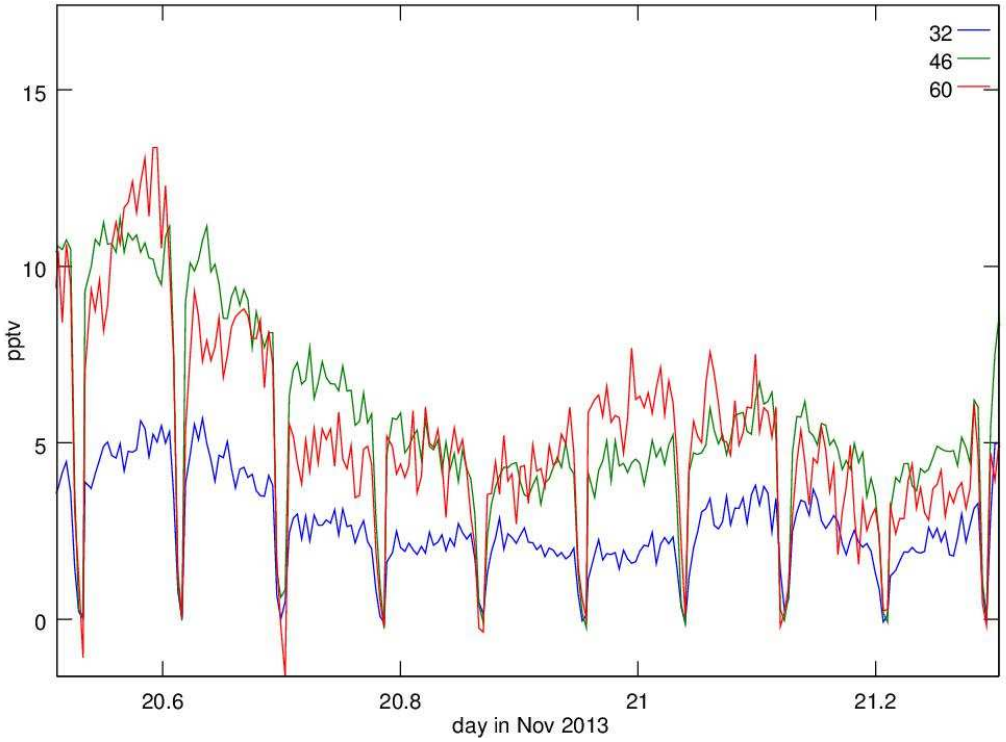

A whole series of tests with the automatic scrubbing procedure are depicted in Figure S5. Net mixing ratios in pptv are shown (zero data is not depicted) for the alkyl amines in ambient air in Minneapolis from the 18th to the 25th of November, 2013. At 19.53 d, the sampling arrangement was changed from catalytic converter zeroing to sampling through the three-way valve with diversion through the scrubber tubes for BG determination every ~2 hrs. There was an initial conditioning period of the three way valve that lasted until about 19.8 day. A 30 cm sulfuric acid coated Teflon tube was used as the scrubber for the first day. On the 20th, this was changed over to a 70 cm phosphoric acid scrubber tube (at 20.4 day.) At 22.64 days, the scrubber tube zeroing procedure was terminated and

the catalytic converter zero was re-established: the three way valve was returned to its position downstream of the catalytic converter.

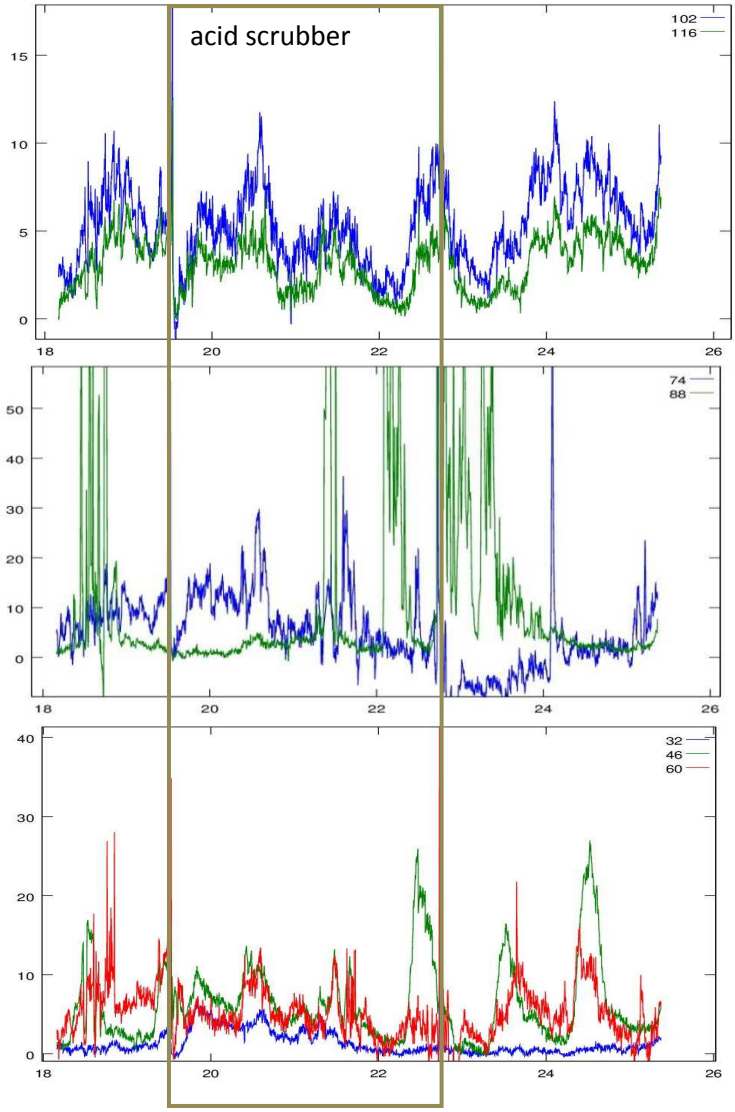

Figure S5. Mixing ratios in pptv vs. day (Nov, 2013, Mpls.) for (a) methyl, dimethyl, and trimethyl amines, (b) C4 and C5 amines (or C3 and C4 amides) and (c) C6 and C7 amines (or C5 and C7 amides). Between 19.73 and 22.75 day an acid scrubber tube was used to obtain instrument zeroes. Before and after that, the catalytic converter zero was used.

The mixing ratio data (pptv in the figure) show no discernible difference for the alkyl amines whether using the acid scrubbing tube or the CC zero, with the exception of mass 74 especially after the CC zeroing procedure had been restarted. Note that the three way valve had been exposed to outdoor air for the three days it was used in the automatic scrubbing arrangement and it could have become a small source of the amine at 74 u when retasked for automatic CC zero-ing. An amine mass spectrometer, recently described by Yu and Lee *(2012)*, has also used an acid scrubber, based on silicon phosphate/H_3PO_4, such as used for ammonia (Nowak et al. *2006*). The results depicted in the figure show that the acid scrubber deployed here acts similarly to the catalytic converter zeroing procedure.

SI 1.4 Response times

An effect related to that detailed above is the interaction of amines with conditioned surfaces in AmPMS. Two experiments are detailed in Fig. S6a and b with (a) dimethyl amine and (b) triethyl amine added to humidified (~30% RH) clean nitrogen into a short sample line (30 cm) before entering the inlet to the drift region of AmPMS. Also shown in the figures are triple decay curves with time constants of

0.33 min, 5 min, and 1 hour. The relative contributions of these three curves are 70 %, 20 % and 10 %, respectively. In Fig. S6b the dimethyl amine spike (green) is shown and during this time some triethyl amine is carried in from the ~ 30 cm length of sampling lines and teflon tee and/or driven off of surfaces within AmPMS.

Fig. S6. Addition and quick removal of (a) dimethyl amine and (b) triethyl amine to AmPMS. The degassing of triethyl amine from surfaces (both internal to AmPMS and the addition tee and lines leading up to it) is apparent during the DMA addition at 16.83 hr. Note that the triethyl amine permeation tube has not been well quantified and these 'spikes' were not calibrations.

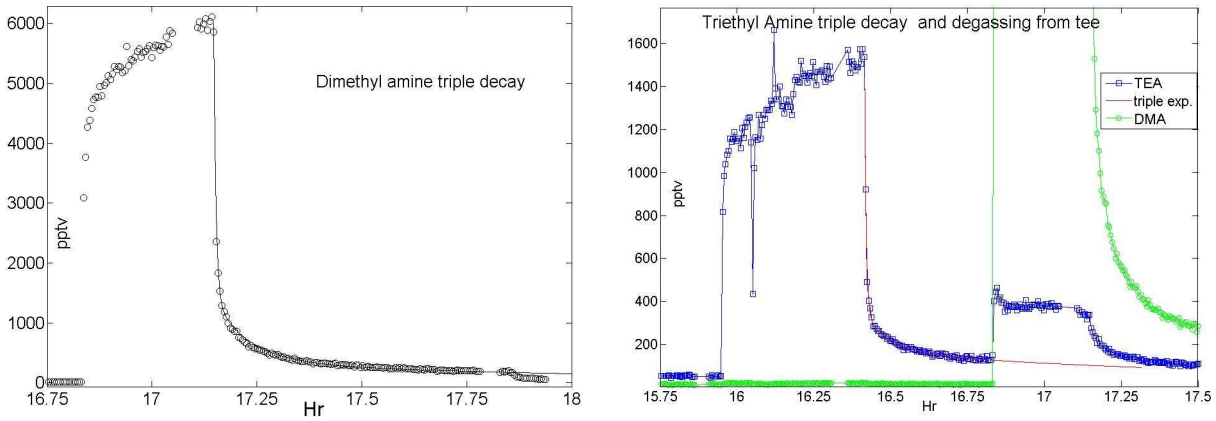

We observed that the method in which the flow from the permeation tube was introduced into the sample flow was important for the calibrations. The best performance was when the entire sample flow was directed over the permeation tube as was done for the majority of the calibration results presented in Table 2 of the paper. The data depicted in S6a and b were performed by tee-ing into the sample flow with a small (~40 sccm) flow from the permeation tube: often, the full amount of amine was not delivered to AmPMS and also degassing effects were larger after another amine was swapped in, such as at 16.85 hr in S6b. Sticking inside tees is probably larger than in smooth tubes because of the junctions and small dead spaces within the tee.

In some cases it appears that ammonia is worse than the amines in terms of sticking. Shown in Fig. S7 is an experiment where ammonia and dimethyl amine were introduced to the AmPMS sample line via teeing into it with the exit of the dilution system. A zero occurred at 13.7 to 13.8 Hr and at ~ 14 hr the dilution system was taken off the mixing tee and replaced with a plug. While both DMA and NH_3 responded quickly to a zero, reflecting rapid response within the AmPMS drift region, NH_3 decayed much more slowly than DMA after the dilution system was removed, indicating sticking of NH_3 on the Teflon lines preceding AmPMS.

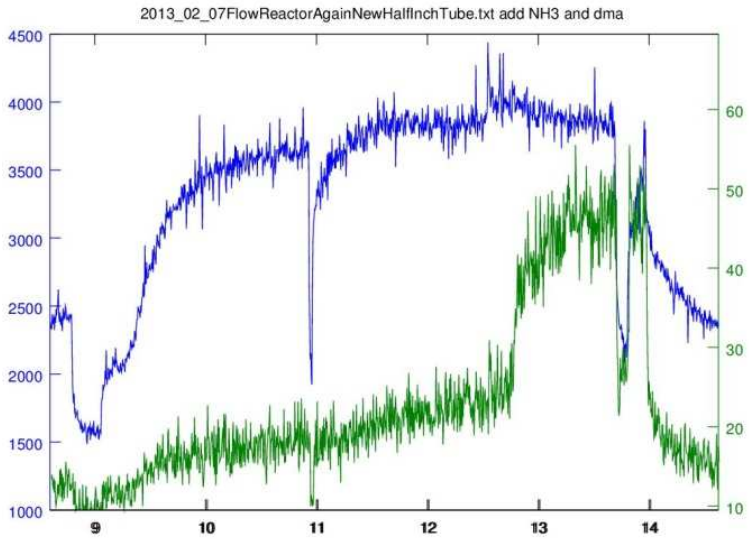

Fig. S7. Co-addition of DMA (green) and NH_3 (blue) to AmPMS. Addition was started at about hour 9, the DMA content was increased at about hour 12.67, and the dilution system was removed from the sample flow at about 13.9 hr. The tail in the NH_3 data indicates a significant degassing from surfaces, likely upstream of the ion drift region, that dimethyl amine was not subject to.

SI 1.5 Inlet + sample line test.

A series of experiments were performed by adding an amine (a spike) at the upstream end of a 3.75 m length of 0.48 cm ID Teflon (PFA) tubing. This inlet tubing was used in the field missions in both Lewes and in Oklahoma. About 20 % of the amine from the permeation tubes was added to the ~ 1 sLpm sample flow of outdoor air in Minneapolis resulting in spikes of about 2000 pptv of methyl or trimethyl amine for a time period of 20 to 45 min. A smaller spike of 400 pptv trimethyl amine was also performed.

Shown in Fig. S8a,b are mixing ratios of the amines for three cases of amine spikes: (i) green, bypassing the 3.75 m inlet, i.e., spike only into the ~30 cm sample line and two tees, (ii) blue, into the 3.75 m inlet that had been rinsed with deionized water after the Oklahoma campaign and then used for about 5 weeks of sampling urban air in Minneapolis (2 weeks in July 2013 and 3 weeks in Oct and Nov 2013) (iii) red, after the 3.75 m inlet was rinsed with hot tap water, ultrasonically cleaned with a dilute Alconox soap solution, rinsed with hot tap water, rinsed with a ~0.5 l of deionized water, rinsed with a few hundred mL of a ~0.01 M sodium bicarbonate solution and then dried after removing most of the droplets from the baking soda rinse. Leftover from the Oklahoma campaign was a small amount of web-like material, perhaps the start of a cocoon. It was near the upstream end of the inlet and it was not fully removed by the cleaning procedure.

In all cases, the trimethyl amine signals continue to slowly increase after the quick rise upon their introduction, as does the methyl amine spike that bypasses the 4 m inlet. The similarity of the slow rise for all these trials indicate that they are due to processes within the addition tee, the drift region and/or the sample line and zero-ing tee just preceding it. Since the duration of the spikes was different for each trial, time zero in the plots was chosen to indicate when the spike was terminated. The decay in time of the trimethyl amine signal is similar for the three cases, which indicates that although the ~4 m sampling line probably introduces a time delay, the majority of a trimethyl amine spike makes it through readily.

The sample line and tee are made of perflourocarbon, the drift region is glass, the ion source and inlets are primarily stainless steel. There are small step transitions before and within the tee and from the tee to the glass drift region where losses to surfaces may occur. Then, when ambient amines levels drop, they may turn around and be sources. Likewise for dead spaces within the tees and the instrument. Shown in Fig. S8c is a smaller trimethyl amine addition of ~ 400 pptv performed for the same conditions as the red line in Fig. S8b ('60 after cleaning' in Fig. S8b).

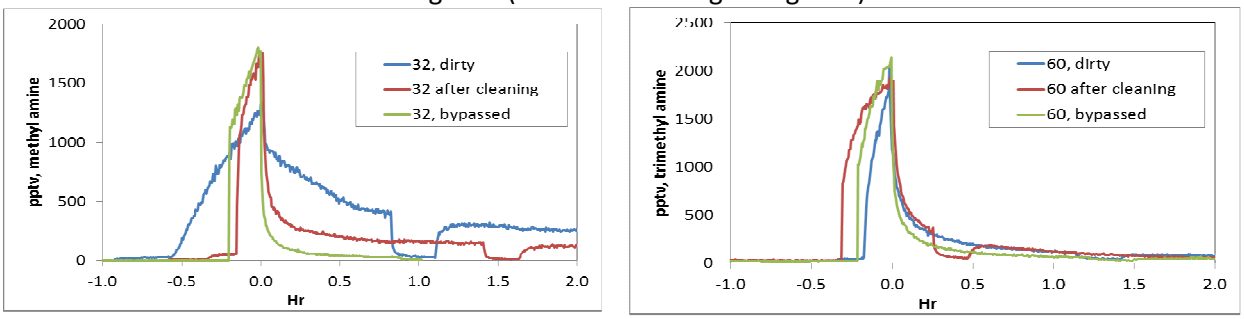

Fig. S8. Rise and decay of methyl amine (a, left) and trimethyl amine (b, right) spikes to AmPMS' 4 m sampling line before and after cleaning and also bypassed.

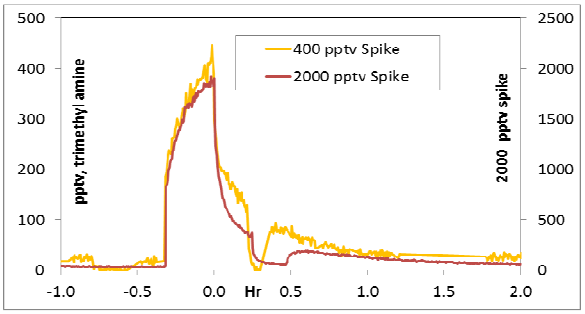

Fig. S8(c). Spike from Fig. S8b shown along with a 400 pptv spike. Time behavior for both spikes is quite similar, particularly on the rise. The decays differ somewhat suggesting a modestly larger effect at smaller amine levels.

There is a prominent interaction of methyl amine with the 4 m inlet line that had been exposed to a large volume of outdoor air (blue line, S8a). Interestingly, trimethyl amine was much less affected by the dirty sampling line. Nonetheless, the data indicates that the inlet absorbs methyl amine, 'passivates' to it on the ten minute (clean) to 1 hr (dirty) time scale, then releases the absorbed material over the next several hours. Catalytic converter zeroes were initiated during the experiments and are easily picked out in the figures.

It appears that the amount of amine added was fully recovered so the effect of the 4 m inlet tubing is to smear out in time changes in ambient amine levels. Therefore the data represents a 'lagging' average in time of the ambient amines (the preceding 10-20 min for trimethyl amine, ~ 1 hr for methyl amine). It is likely that large amines act similarly to trimethyl amine where the effect of the inlet line is significantly muted compared to MA: a ten minute time lag in the data is estimated for changes in amines of 50 %. Since a similar interaction with the drift region and sample line for dimethyl and triethyl amines is shown in Fig. S6a and b, it is probable that dimethyl amine acts similary to trimethyl amine and the larger amines. Ammonia and methyl amine have the largest interactions with perflourocarbon tubing, the glass drift region, and/or the stainless steel ion source and ion inlet. For these reasons and because of the sluggish behavior of the zeroes, the data sets for both Oklahoma and Lewes are reported as ~2 hr averages (some of the later Lewes data is hourly due to more frequent zero-ing.) Note that for much of the time, the response of AmPMS for the larger amines (C3 and larger, probably also C2) is much quicker than 1 hr.

SI 1.6 Detection limits.

We report a detection limit for each amine due to counting statistics as equivalent mixing ratios at 3 times the standard error of the mean of a typical zero signal level. A zero near the middle of each campaign was selected (2012Aug01 for Lewes and 2013May01 for Oklahoma) and the standard deviation of the zero data that was used (the last third) was divided by the square root of the number of data points (19 for Lewes about 10 s of accumulated ions counts, 31 for Oklahoma, about 15 s). Finally, this number was multiplied by 3 and then divided by S_{typ} (about 4 Hz/pptv). These are taken to be detection limits (DL) for ~10 s intervals and are listed in table S1.

In Lewes the instrument background count rate was high at 46 u thus the largest DL for that campaign is for the C2 amine. The background at 46 u was lower for the Oklahoma deployment however mass 74 had a very high background count rate and thus the highest DL. Note that amines were generally very high in Oklahoma and limitations due to counting statistics were not important for detecting ambient amines. The DLs listed in the table were taken from zeroes in the middle of the campaigns and the DL for a particular amine can vary from these values. It is important to note that the ambient data was averaged over hour long (up to 8 hr) periods and that detection of amines below these 10 s DLs is not only possible but was routine.

Table S1. Typical detection limits in pptv from statistical considerations. Data averaged over one or two hours has two background determinations, one before and one after, and is in principle lowered by a factor of $1/2^{0.5}$.

	time	32 u	46 u	60 u	74 u	88 u	102 u
Oklahoma (pptv)	10 s	1.9	7.5	5.6	16.2	4	4.6
Lewes (pptv)	10 s	4.1	13.5	2.7	3.3	2	2.6
Oklahoma (pptv)	1-2 hr	1.3	5.3	4.0	11.5	2.8	3.3
Lewes (pptv)	1-2 hr	2.9	9.6	1.9	2.3	1.4	1.8

SI 1.7 Interpolation between BG determinations.

There were variabilities in the zero values that were due to quick changes in RH. These variabilities were not fully captured by the interpolation procedure (cubic spline, the 'spline' function in Octave / Matlab). This led to a large number of false negatives in the five minute Lewes data for

ambient amines at low concentrations. Shown in Fig. S9a are the pptv values of the background levels at 46 u (light blue circles) measured in Lewes for a 4.5 day period in August, 2012. The data shown here contain some of the most numerous and sizeable false negative 5 min data. The connecting light blue curve is the spline BG interpolation used to obtain net mixing ratios for DMA, which are shown as the red symbols. Many false negatives are exhibited in this data set and the appearance of these artifact variations in net mixing ratios is well correlated with variations in RH and the ratio of signals at 55 u and 37 u (the $H_3O^+ \cdot 2H_2O$ and the $H_3O^+ \cdot H_2O$ ions, respectively) a proxy for RH, shown as the bright red line (right scale.) Note also that the changes in the BG level of 46 u correlate well in time with the changes in the 55 u to 37 u signal ratio.

These RH induced artifacts in DMA are due to the interpolation scheme. Including a dependence on RH in the interpolation scheme was not readily achieved because the overall day-to-day BG level was not well correlated to water content over the whole campaign, despite the clear correlation of the changes in RH with the perturbations in the 5 min data in the figure. For the Lewes campaign, RH variations were relatively rapid and the ammonia, MA and DMA data were rendered as 4 or 8 hour averages. When the data for the Oklahoma campaign were hourly (or two-hourly) averaged, most of the false negatives disappeared; a few still remain in Figs. 5 and S10b. Ambient measurements in Minneapolis (see Fig. S4b) and Atlanta (five min data presented in Hanson et al. 2011) were not impacted by variations in RH because these variations in time are modest in Minneapolis and the humidity of the source flow gas in Atlanta was more or less independent of ambient humidity levels.

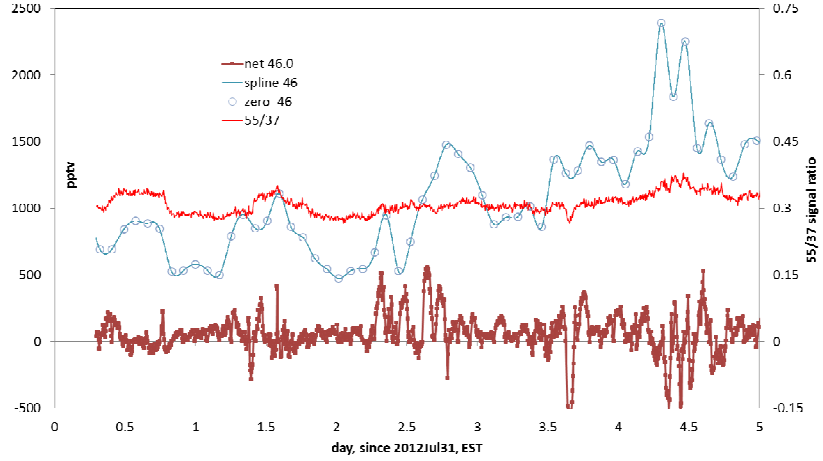

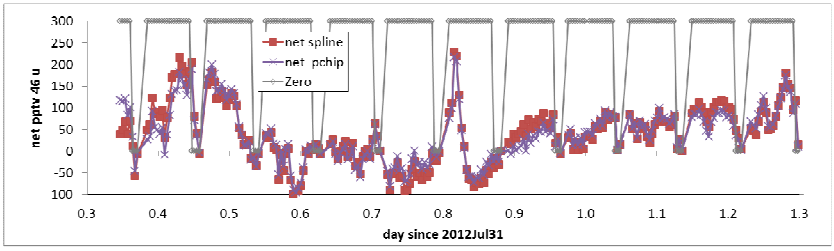

Figure S9. (a) Above, background equivalent and net mixing ratios for DMA and signal ratio for 55 u to 37 u, Lewes DE. (b) Below, blowup of net mixing ratios in (a) for DMA showing two different background interpolation schemes.

The choice of interpolation scheme affects the net amount of DMA during times with relatively rapid changes in RH. This is shown in Fig. S9b where net DMA mixing ratios (5 min average values on 2012Aug01) using a spline interpolation scheme and the pchip interpolation scheme are compared: the difference can be up to 50 pptv. The times when zeroes were determined are indicated by the gray line at zero. The difference in the 1 or 2 hourly averaged data using the two interpolation schemes is generally much less than the differences in the 5 min data shown in Fig. S9b. The long-time averaged data (1, 2, 4, and 8 hr) had very few false negatives.

SI 1.8 Low ion count rate episodes.

There were episodes during the OK field study where the instrument had very low reagent ion count rates and its absolute detection sensitivity had been debilitated. Some calibrations for methyl amine and DMSO were taken when the instrument had been in one of these episodes. These episodes occurred, presumably, when there was a clog in the ion entrance orifice (e.g., dust or fiber) that lead to

large reductions in ion signals (up to 97 % decrease in s_0 ~ 3000 Hz). In these cases, the relative sensitivities for CH_3NH_2 and DMSO, ratioed to S_{typ}, appeared to increase to 3 and 6, respectively, much greater than for nominal operating conditions. Right after these anomalous calibrations had been performed, the orifice clog disappeared when a very hot catalytic converter (660 °C) was placed in line with the sample gas; the data shown in Table 2 of the paper were taken when signals had returned to normal levels, s_0 ~ 100 kHz. The amount of signal loss was variable in the field campaign, reflecting variability in the position of the ion beam and also the degree of orifice blockage. When s_0 was reduced by more than 95 %, the relative sensitivities were probably greatly affected. Therefore, ambient measurements were deemed reliable when losses in s_0 were less than 95 % (e.g., S_O > 5 kHz.) Some calibrations were performed at ~90 % loss reagent signal and were comparable to the normal reagent ion signal calibrations.

SI 1.9 Additional Lewes and Oklahoma ambient data

Presented in the Figures below are the mixing ratios for the latter half of the campaigns in the same format as the first half in the main paper.

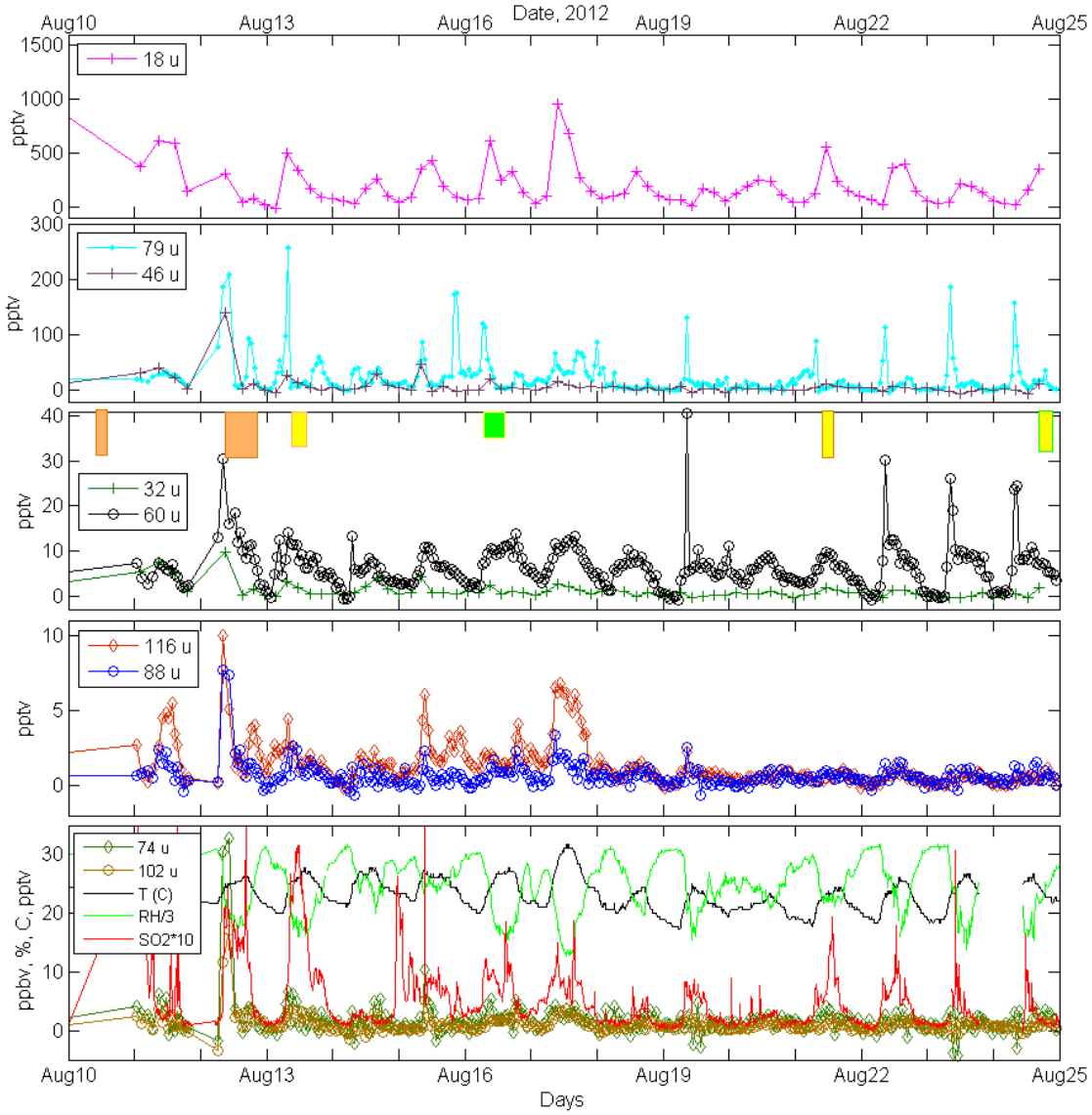

Figure S10a. As in Figure 4 in the text, mixing ratios for ammonia (top), DMA and DMSO (next), MA and TMA (middle), C5 and C7 amines (bottom middle) and C4 and C6 amines along with temperature, relative humidity and SO_2 (ppbv*10). New particle formation events are indicated in the middle plot. Time is EST.

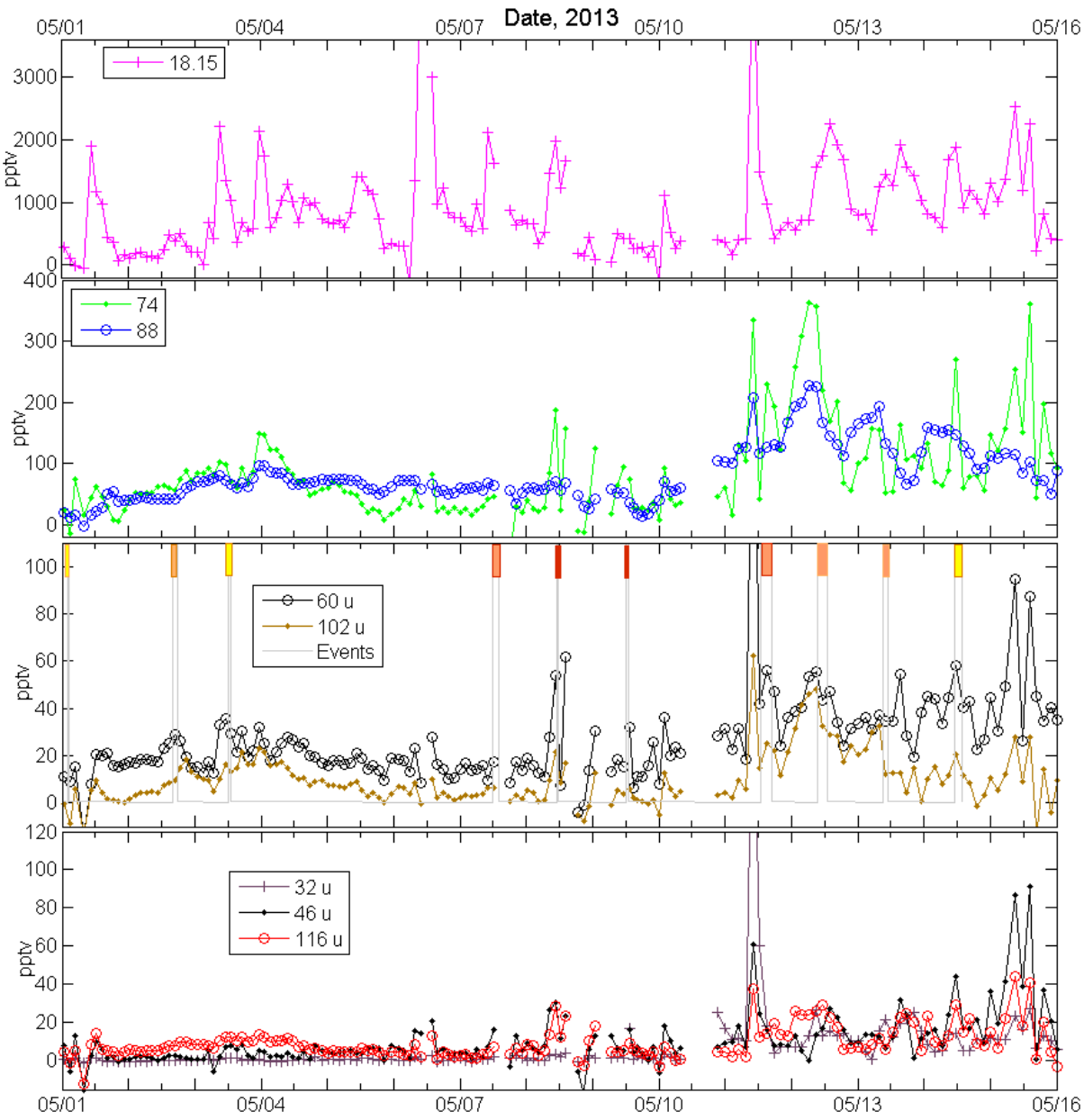

Fig. S10b. As in Fig. 5 in the text, ammonia (top), C4 and C5 amines (top middle), TMA and C6 amines (bottom middle) and MA, DMA and C7 amines (bottom.) New particle formation events are indicated in the 3rd plot down. Time is CDT.

SI 1.10 Atlanta data and analysis of Lewes and Oklahoma data sets

Because of the BG interpolation issue with the Lewes data and the sluggishness in the Oklahoma data, a potential systematic uncertainty of +100/-50 % applies to these data sets. Added (geometrically) to the +/- 30 % uncertainty in the calibrations, and the overall uncertainty is +150/-60 %. The Atlanta amines data set published in Hanson et al. (2011) does not suffer from either the sluggishness in zero determination nor the BG interpolation problems. The negative values in the 5 minute amine data previously published are up to a few pptv and are less than the detection limits.

Future work with the Lewes data sets will involve tying the background interpolation scheme to relative humidity, absolute water content, and/or the proton water cluster signals which are a proxy for RH. For the Oklahoma data set, fits to the time dependency of the sluggish data (i.e., exponentials) will be attempted to more fully ascertain any bias in the net amine levels.

SI 2. Calibration of AmPMS with VOCs

DMSO was detected in Lewes DE by AmPMS; it has a large proton affinity and detection by mass spectrometry has been reported by Nowak et al. *(2001)* A DMSO PT was fabricated and its permeation rate was determined by comparing it to an evaporation calibration of a PTrMS (see below). Detection of DMSO by AmPMS was primarily as $DMSO{\cdot}H^+$ at 79 u but a signal at 96 u due presumably to the $DMSO{\cdot}NH_4^+$ ion, tracked the signal at 79 u. This is depicted in the figure below where the signal ratio of 96 u to 79 u is plotted against the signal ratio of 18 u to that of the water proton clusters (19 u, 37 u and 55 u). Evidently, DMSO reacts with $NH_4^+{\cdot}(H_2O)_n$ clusters and retains the NH_3 ligand to some extent.

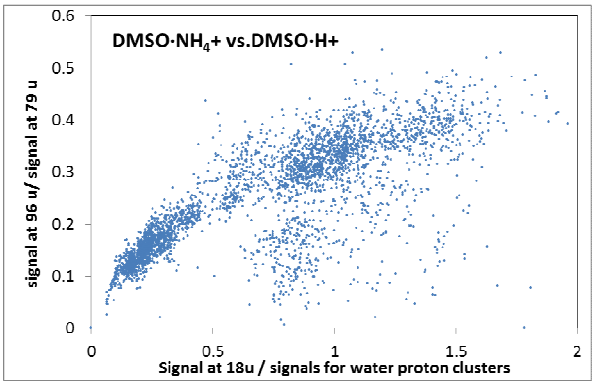

Fig. S11. Signals due to DMSO reacting with water proton clusters and ammonium clusters (18u).

SI 2.1 DMSO quantification.

A DMSO permeation tube was quantified by comparison to a calibrated PTrMS (Hanson et al. 2009). The PTrMS was calibrated for DMSO by the evaporation method. In the PTrMS calibrations (two evaporation trials are shown in Fig. S12), the DMSO signal at $M{\cdot}H^+$ (79 u) was accompanied by signal for dimethyl sulfone ($DMSO_2$) at $M{\cdot}H^+$ = 95 u. DMSO is a sticky molecule and is retained for some time on the PTrMS sampling lines and within the ion drift tube. When it is stuck on the surfaces in the drift tube it is exposed to OH radicals from the glow discharge ion source. DMSO residing on the inner surface of the drift tube is apparently readily oxidized to $DMSO_2$ (A. Wisthaler, private communication, 2013) and perhaps other species: e.g., the main gas-phase product is methane sulfinic acid (**S29**). The sum of the signals at 79 u (37%) and 95 u (63%) were used to obtain sensitivities and to transfer these sensitivities to quantify the permeation tube; if DMSO oxidizes to any other species, then the permeation rate is underestimated.

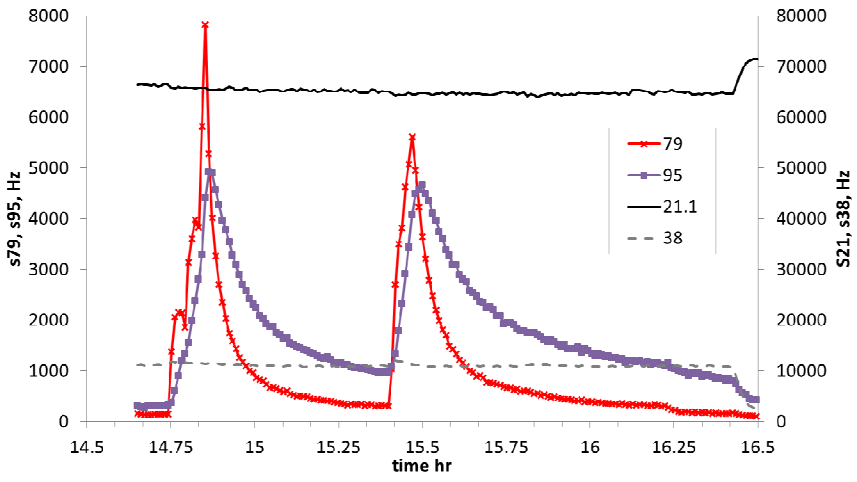

Fig. S12. PTrMS signals due to DMSO and its oxidation products within the PTrMS instrument. Two evaporations of uL quantities of mM DMSO solutions into a carrier gas sampled by the instrument are shown.

When the DMSO permeation tube was used to calibrate AmPMS, there was no signal observed at 95 u. This is consistent with low amounts of OH exiting the radioactive ion source of AmPMS (vs. the PTrMS' glow discharge source) and the much lower sticking observed for DMSO when introduced into AmPMS. Note that the DMSO permeation rate is uncertain due to potentially undetected oxidation products inside the PTrMS drift

tube. To remedy this situation, gravimetric determination of the DMSO permeation rate and DMSO evaporation calibrations of AmPMS are planned.

SI 3. Other ions observed in Lewes campaign.

There were a number of ions that do not correspond to alkyl amines that were monitored at each site. They are difficult to assign to any particular species and thus have unknown sensitivities however, assuming efficient proton transfer, observed net signal can be converted to mixing ratio using S_{typ}. A few ions with interesting behavior observed at Lewes DE are depicted in the figure below along with the signals due to DMSO. If they are due to species with amino groups they are likely to be detected quite efficiently (i.e., it is appropriate to convert signals to mixing ratios assuming S_{typ}.) Early in the campaign, sp168 (the species detected as 168 u) was generally quite low while sp186 was at times 40 pptv. Later on in the campaign, they were at comparable levels and well correlated; they were generally high during the night and low during the daytime. With the exception of pyridine at 80 u (with a little spillover from C-13 DMSO), these species cannot be readily identified and it is possible that the signals represent more than one species: among a number of species, 168 u could be protonated ring amine compounds species such as carbazole or cyclohexyl piperidine or oxidized species such as dipicolinic acid and methoxyanthranilic acid. This is an example of some of the additional ions besides those due to the alkyl amines that arise from sampling ambient air, as detected using AmPMS. Even though the ions at 168 and 186 u are not assigned to any compounds, they are shown here as they show a significant correlation with DMSO for the last 12 days of the 2012 campaign in Lewes, DE.

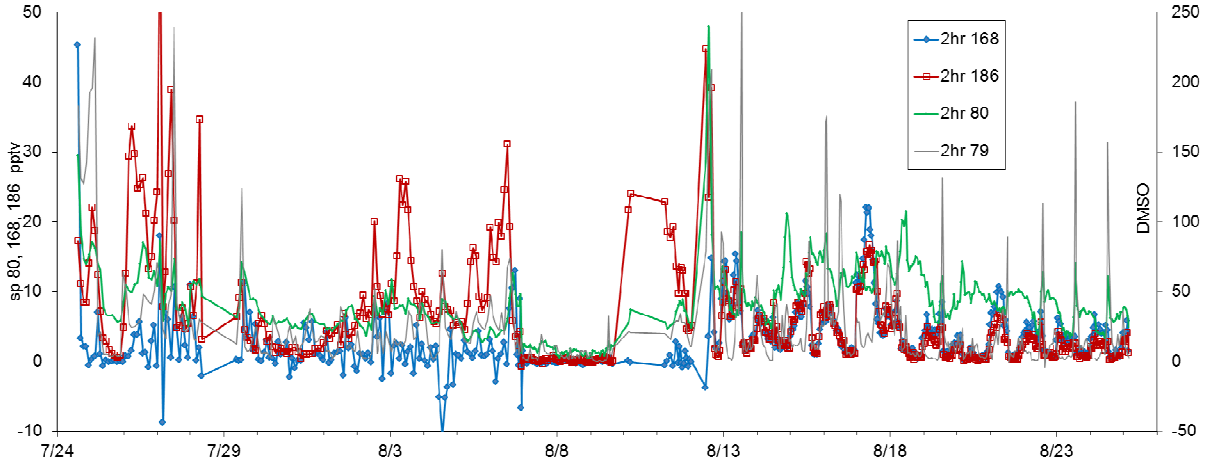

Fig. S13. Species due to ions detected at 80, 168 and 186 u along with 79 u (right axis, due to DMSO.) Signals converted to mixing ratio, pptv, assuming S_{typ}.

Table S2. Masses that showed significant net signals during the Lewes campaigns.

Detected Mass, u	Species Identity, assuming M•H$^+$	Note or alternative species
18, 32, 46, 74, 88, 102, 116	NH_3 and the alkyl amines	Amides
79, 96*	DMSO	* DMSO•H$^+$ + NH_3 ligand
80, 94	Pyridine, methyl pyridine	
59, 101	Acetone, C6 enol [a]	Acetone sensitivity is low
121, 135	Tri-, tetra-methyl benzene [a]	Markers of indoor air contamination
168, 186	Carbazole, methoxyanthranilic acid[a,b]	186 could be water + 168…
44	Cyanuric acid	TMA oxidation product [c]

[a] Tentative but probable and sensitivities unknown. [b] Examples from a long list of potential species.
[c] Onel et al. (*S36*) report the formation of methyl methanimine from oxidation of trimethyl amine.

SI 4. Diurnal hourly means, medians and percentiles, Oklahoma.

Discussed in the text are the diurnal behavior of the medians for amines and ammonia from Oklahoma. Shown below are the plots for ammonia (18 u), methyl amine (32 u), and dimethyl amine (46 u) are in the left hand plots; C3 amine (60 u), C4 amine (74 u) and C5 amines (88 u) are in the middle plots, and C6 and C7 amines are on the right. Data are plotted as mixing ratios (in pptv) against hr of the day. The 25th and 75th percentiles are also depicted.

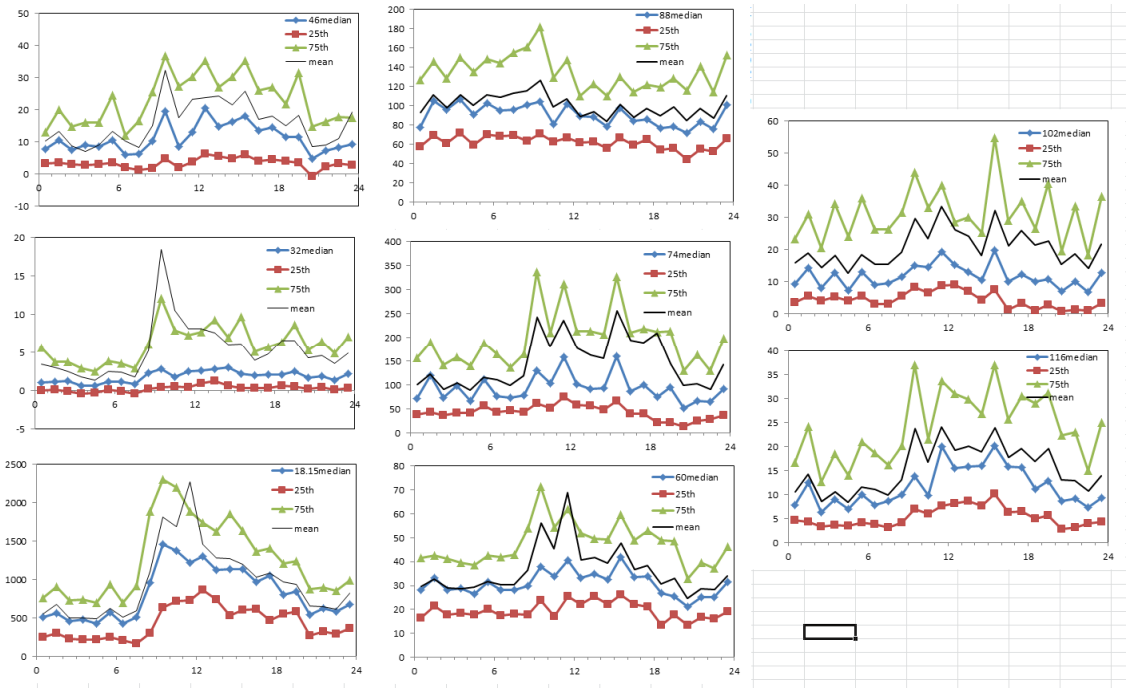

Fig. S14. Diurnal hourly mean, median and 25th and 75th percentiles for ammonia and the amines detected in Oklahoma, Spring 2013.

SI 5. Correlations from Lewes

Ammonia, methyl, and dimethyl amine data from Lewes are shown in correlation plots below (Fig. S15a-b). Methyl and dimethyl amines are well correlated, ammonia and methyl amine are somewhat correlated and the C4 and C6 amines (S15c) are well correlated. Other species of note in the Lewes data set is trimethyl amine which was not correlated with any other amines but was somwheat correlated with DMSO (79 u).

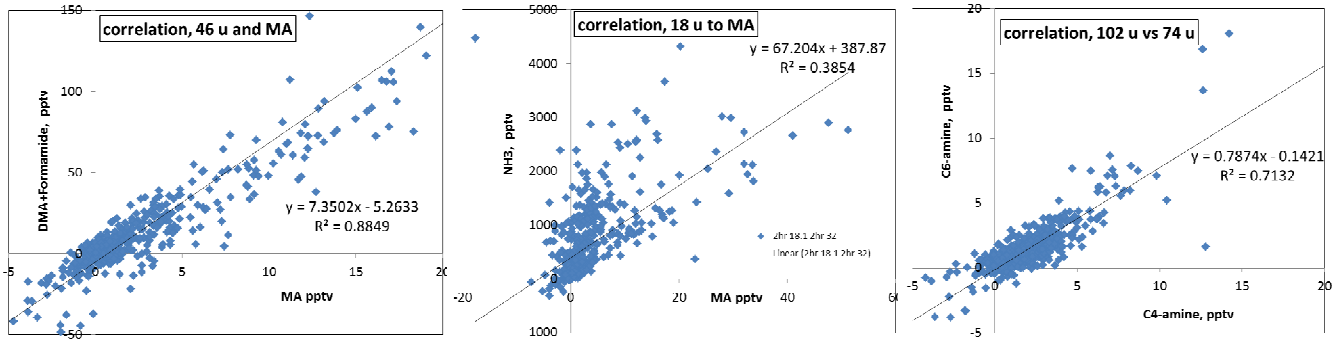

Fig. S15a-c. Correlations of DMA with MA, NH3 with MA, and the C4 and C6 amines.

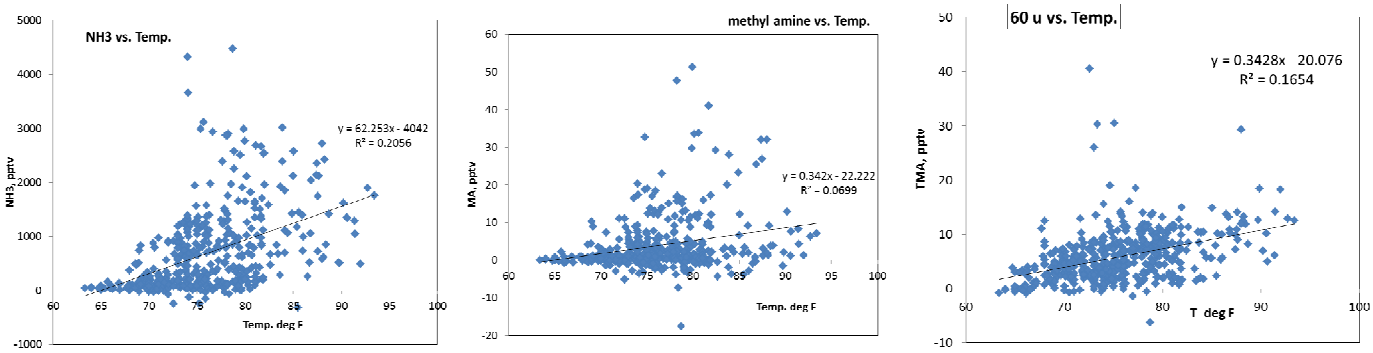

Fig. S15d-f. Correlation plots of ammonia and MA and TMA with temperature. R^2 is the square of Pearson's correlation coefficient. Ammonia and TMA show a modest correlation with temperature.

SI 6. Addition of Base to a Flow Reactor and Computational Fluid Dynamics.

Amine levels needed for nucleation studies *(Zollner et al., 2012; Kirkby et al. 2011)* are in the single to tens of pptv range. To achieve this in a flow reactor experiment operating at 3 to 4.5 mmol/s total flow, the flow from the PT was diluted in multiple stages with an overall decrease of up to 99.9% of the amine. Amine levels of several hundred pptv in a flow of ~50 sccm N_2 were prepared with the dynamic dilution set-up shown in Fig. S16a and delivered to the flow reactor through a sidearm (S16b) and further diluted by the total flow (6000 sccm or 4.5 mmol/s) to single digit pptv levels. Note that the flow reactor wall is coated with H_2SO_4 and is a sink for bases. Therefore, there is not a uniform [base] present after mixing; however, a useful reference is the mixing ratio calculated assuming No Loss and after Dilution (NLD). During mixing, [base] is quite a bit larger than NLD; on the other hand, near the walls or at the end of the flow reactor [base] is much less than the NLD value *(Zollner et al. 2011)*.

Previously, ammonia or methyl amine was introduced to the flow reactor between the mixing region and nucleation region shown in Fig. S16b (Zollner et al. 2011). Without dilution of [amine], particle numbers saturate the particle counter thus the need for low levels in the nucleation region. The base level at the detection region of the flow reactor (~ 120 cm downstream) was very low due to loss to the wall. In some experiments, the dilution system was connected to a port at the bottom of the flow reactor and AmPMS signals were in agreement with that expected for NLD.

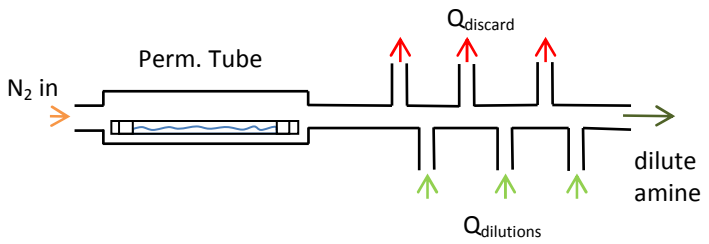

Figure S16a. Dynamic dilution set-up. Nitrogen gas is sent over the PT and then known fractions of gas are removed and then replaced by clean N_2. The amine level is diluted several times before interring the flow

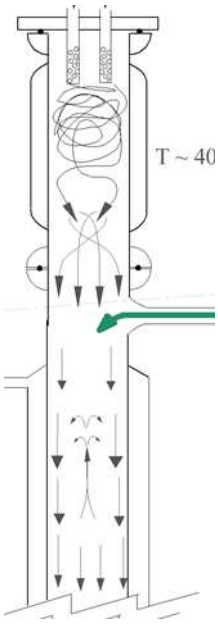

Figure S16b. Base addition port on the nucleation flow reactor. The flow from the dilution system mixes with the nearly plug and warm (~30-35 C) flow within ~20 cm; simulations show that this addition eliminates much of the buoyant zone flow.

Computational fluid dynamics simulations of the mixing of the base into the main flow were performed using the 3D model of Panta et al. *(2012)* with the following important alterations: (i) the number of volume elements was increased from $1.4x10^5$ to $2.1x10^6$, (ii) second order solvers were selected for energy, momentum, pressure and the monomers (sulfuric acid and base) and (iii) the convergence criteria for many parameters were strengthened.

Shown in Figs. S17 are contour plots of (a) ammonia addition into 6 sLpm through the top port as shown in Fig. S16b and (b,c) dimethyl amine addition to a flow of 4 sLpm near the bottom of the flow reactor. The ammonia levels shown in S17(a) agree with those of our previous fluid dynamics simulations shown in Fig. A11(II) of Panta et al. *(2011)*: the main difference is that the improved 3D model here has the sidearm flow, and thus ammonia, better traverse into the center of the reactor. The current results are in accord with the conclusion of the previous work where it was shown that

mixing is sufficiently fast such that the majority of nucleation occurs at least 10 cm downstream of the base addition port (Figs. A12 and A13 in the Appendix of Panta et al.) The maximum in concentration 18 cm downstream of the port is about twice the NLD value; the average value across the diameter of the flow reactor is about the NLD value.

Figure S17a. Contours of ammonia (24 pptv intervals, 240 max). NH_3 in a sidearm flow of N_2 (0.05 sLpm) added to the main flow (6sLpm) that is also cooling due to interacting with the wall: from 307 K (incoming at the left) to ~298 K (outgoing, right.) NLM is 16 pptv. Note that ammonia is present at ppbv levels in the N_2 flow (40-100 sccm) exiting the dynamic dilution system, and it mixes down to the tens of pptv levels in the main flow.

The dynamic dilution system was also attached to the flow reactor near the flow reactor exit and just above a mass spectrometer system which monitors trace species using chemical ionization with NO_3^- or H_3O^+ core ions (as in AmPMS and *S30, S31, S35*). The distance between the port where the dynamic dilution system enters the flow reactor and where the mass spectrometer samples the flow is 18 cm. Experiments on the formation of H_2SO_4 dimers have been recently published using this arrangement (S32). Here we report supporting CFD simulations of amines, H_2SO_4 and their clusters. The total flow rate in the reactor is 4 sLpm, the total flow from the dynamic dilution system is 40 sccm, the base is dimethyl amine (estimated diffusion coefficient in N_2 of 0.11 atm cm^2/s) and temperature is 298 K.

The results of the simulations (Fig. 17(b)) show that mixing of base into the sulfuric acid containing flow is similar to that shown in 17(a) for ammonia. The main difference is that the sidearm flow is not as penetrating in the isothermal case (17b) which is probably due to the lack of a central buoyancy that allows for more flow at the center. Nonetheless, whether the mixing occurs at the top of the reactor near a buoyant flow or into an isothermal, but smaller, flow, mixing via diffusion is relatively rapid. Reverse pathlines beginning at the center of the sampling region of the mass spectrometer and ending at the level of the base inlet show that there is about 2-to-3 s of reaction time for the 18 cm of travel. This average velocity is about twice that assuming plug flow: this is expected for the centerline flow for fully developed laminar flow.

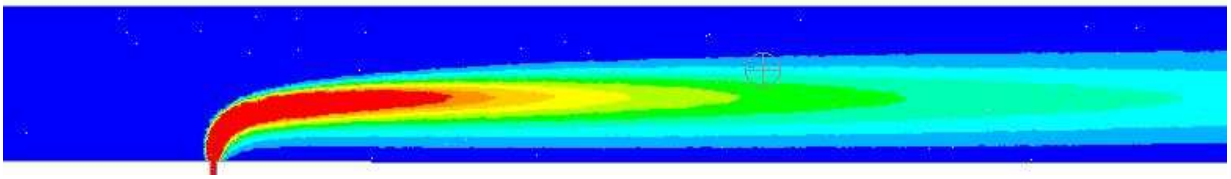

Figure S17b Contours of dimethyl amine (intervals, 2.5 pptv, 25 max). Amine in a sidearm flow of N_2 (0.04 sLpm) added to the main flow (4 sLpm) for isothermal conditions (298 K.) NLM is 5 pptv.

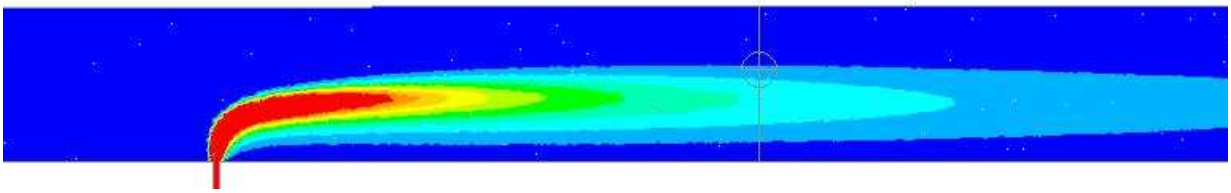

Figure S17c. Contours of dimethyl amine as in (a) but now allowing it to cluster with sulfuric acid molecules, present at ~50 pptv. Differences with S17b is due to uptake onto clusters.

Fig. S17c shows DMA contours allowing for reactions with sulfuric acid. It shows that at ~18 cm downstream of the port (the gray line and circle +), DMA has a maximum of 7 pptv which is about 5 pptv less than the maximum when no reaction is allowed. The reaction scheme will be presented in a

manuscript under preparation (*S33*). The no-loss mixing ratio (NLD) for his simulation is 5 pptv. The simulation shows that sulfuric acid is about 50 pptv in this region of the flow reactor: sulfuric acid is also lost on the reactor wall and has a maximum value on the central axis of the flow reactor.

SI 7. Permeation Tube and Titration Information.

Shown in Fig. S18 is a schematic diagram of two small flasks (in tandem arrangement) with stirring bars, pH probes, and bubbling permeation tube gases. Stirring enhances the presence of acid at the surface of the bubbles, ensuring better transfer of base gas into solution. Flow rate of N_2 over an NH_3 permeation tube was varied from 5 up to 40 sccm and there was no noticeable effect on the measurements.

SI 7.1 Tandem titration

Figure S19 shows data from a tandem titration where base absorption rates for both flasks are shown. The first solution (red) shows an NH_3 absorption rate (13 pmol/s, ~2 year old PT) while the second solution (black) absorption rate is much lower (0.7 pmol/s) during this time. These data indicate that the first flask captures 95 % of the base molecules in the flowing gas. Blank runs (without a PT) showed generally low but at times quite variable neutralization rates: as low as 0.5 pmol/s and as high as 3 pmol/s; sometimes the initial (first 1000 s) neutralization rate was even larger. Absorbed base on silicone sealing materials and Teflon components are believed to be responsible for this artifact neutralization. The high rates were traced to previous exposure to base at high levels: thorough cleansing of the entire apparatus was important. Therefore, the carryover from the first flask for pH < 6 is probably less than 5 % and no correction to measured neutralization rates have been made for this effect.

After the first solution had been neutralized, the rate of absorption by the second flask slowly increased and reached a maximum of ~4 pmol/sec. This delay and the overall slower neutralization rate were due to the saturation of the first solution according to NH_3's Henry's law solubility after the acid had been used up. The time delay in the pH changes in the second solution is roughly in accord with an estimated time constant for Henry's law saturation of the first solution, ~$1x10^5$ s, given by the quantity HRTV/F where H is the Henry's law constant (60 M/atm(***S34***)), R is the gas constant, T is temperature, V is the volume of the solution and F (~22 cm^3/min) is the volumetric flow rate of the PT assembly.

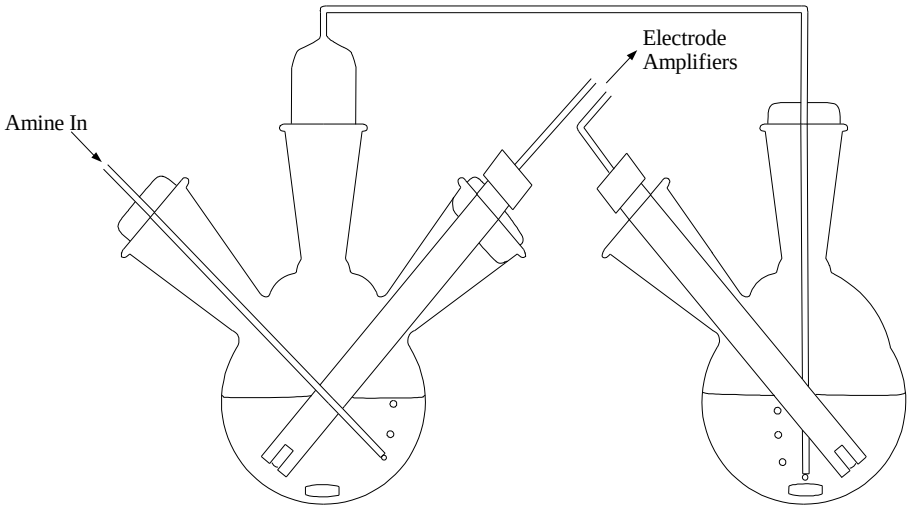

FigF

Figure S18. pH measurement apparatus. Effluent from perm tube at 20 sccm is bubbled through a stirred 40 mL solution initially at pH 5. Tandem apparatus is shown for assessing carryover; generally these two flasks are run in separate experiments and two amine PTs can be calibrated simultaneously.

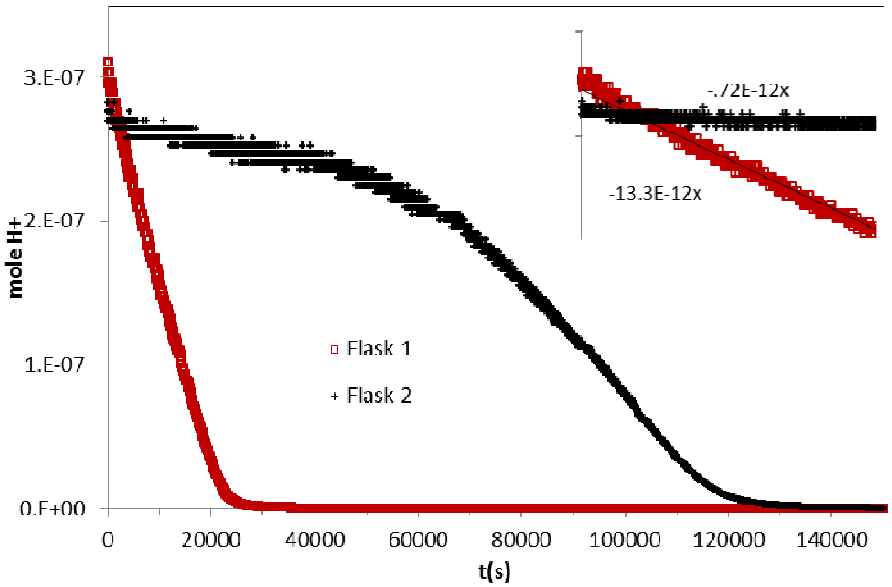

Figure S19. A tandem titration of an NH_3 PT. Mole H^+ vs. time where red squares represent the first flask and the black symbols (+) represent the second flask. The initial 10000 s are shown in the inset.

SI 7.2 Time and Temperature dependence of Permeation Rates

The change in the permeation rate with time of a newly constructed dimethyl amine PT was investigated and after about two weeks the permeation rate had stabilized (Fig. S20). This may be a common behavior for our PTs and it is probably due to the time that is needed for the steady state flux through the wall of the PT to be established. It may also be due to chemical conditioning of the plastic. Permeation rates for some PTs decreased steadily over time (Fig. S21) possibly due to the loss of the amine inside the tube; others maintained fairly steady rates for many months. Water also probably permeates from the tubes for those amines in aqueous solutions and thus changes in composition over time may occur which may be responsible for some of the time dependent permeation rates. The amount of water loss was not assessed (which is probably difficult to do when the PT contains mixtures).

Frequent calibrations are necessary to capture the day-to-day variability in the permeation rates. For the mature PTs depicted in Fig. S21, the exponential fits to the amine PTs are included to guide the eye rather than to explain the data. The several month old NH_3 PT in the figure had a perm. rate of 120 pmol/s which decreased to 60 pmol/s over ~3 mos. and over the next 5 mos. its perm. rate varied between 50 and 80 pmol/s. It has a rather large day-to-day variability that is about ±25 % (the very large value at ~220 d was when the room was quite warm.) The very mature DMA PT in the figure had a rate that decreased from 15 to 6 pmol/s over 120 days - a rather quick secular change and this PT was taken out of service. MA decreased from 40 to 20 pmol/s over a 100 day period but it became more stable over the next few months at 12 to 15 pmol/s. Making titration calibrations a routine component of PT work is important.

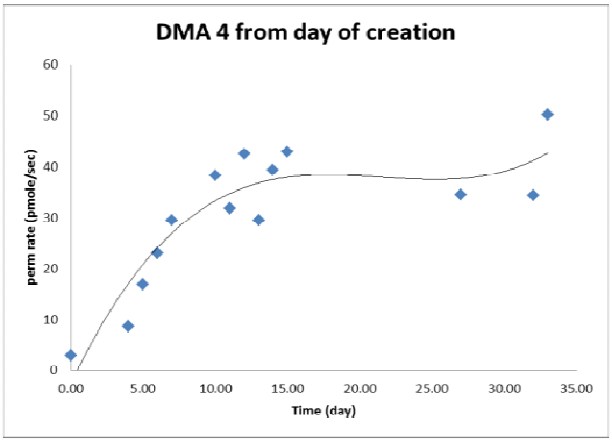

Fig. S20. Permeation rate of a dimethyl amine PT in its first month. Rate stabilized in about two weeks; a mature PT is considered to be one of 1 month age or longer. Perm. rates of mature PTs generally decline slowly with time.

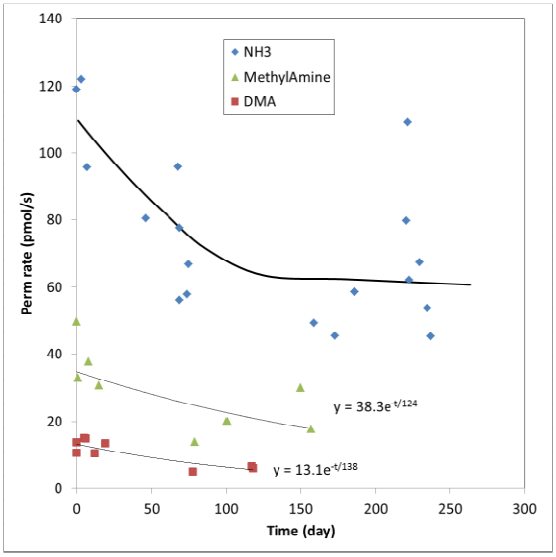

Figure S21. Permeation rates of mature PTs over the course of several months. The lines are drawn to guide the eye and for the amines are exponential decays. The scatter in measured permeation rates can be quite large day-to-day.

Shown in Fig. S22 are permeation rates for a mature NH_3 PT as a function of temperature. A linear relationship with temperature explains the dependence adequately. Near 30 °C, the rate increases about 6 % per °C; this is close to that measured for deuterated acetone *(Brito and Zahn, 2011)*. Another NH_3 PT showed a similar temperature dependence. The PT's time at each temperature was a few to several hours and it is possible that more time is needed to fully establish steady state permeation rates. Nonetheless, this temperature dependency may adequately represent the changes in permeation rates when temperature changes occur on the time scale of several hours.

Certainly part of the day to day variability in Figs. S20 and S21 is due to changes in room temperature which was generally noted to be within 3 ° of 25 °C. PT temperature since then has been routinely recorded along with pH measurements. Temperature stability of the PT during its use is also important. There are some titration experiments where the pH probe had not been recently calibrated and a drift of up to 0.15 pH units in the probe response was noted. This would lead to an error of up to 40 % for these isolated experiments. Calibration of the probe for each titration and checking it post titration is now routine. As discussed above, titrations starting at higher acid content (pH of 4.3 or so) show less variability.

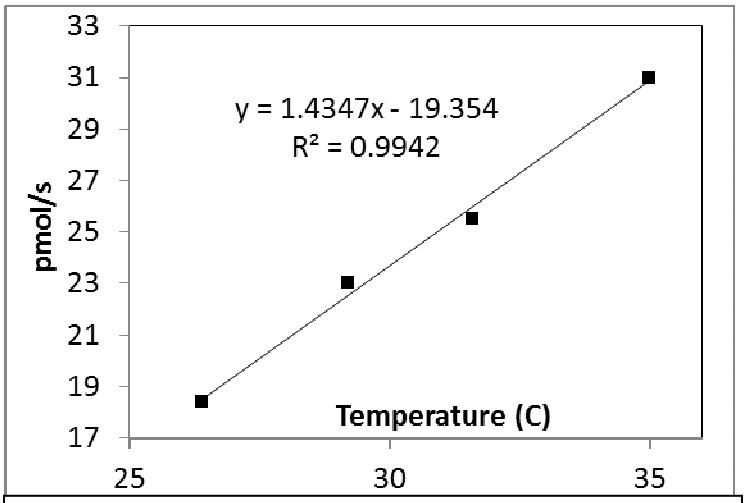

Figure S22. Changes in NH_3 permeation rate with variations in temperature. Increase in permeation rate is approximately linear in this small temperature range.

The large value measured for the NH_3 PT at day 222 in Fig. S21 seems to be an outlier, even considering that the room was warm that day. This is not the only set of measurements that shows this behavior. It is possible that the PTs experience a large and temporary increase in rate of about a factor of two and that last for about a day. These outliers only occur for about 3 % of the measurements and

thus may reflect undetected changes in the measurement apparatus, e.g., pH probe, rather than actual hiccups in the permeation rates.

References for SI.

S29. Arsene, C., Barnes, I., Becker, K.H., Schneider, W.F., Wallington, T.J., Mihalopoulos, N. and Patroescu-Klotz, J. Formation of Methane Sulfinic Acid in the Gas-Phase OH-Radical Initiated Oxidation of Dimethyl Sulfoxide, Environ. Sci. Technol., 36, 5155-5163, 2002.

S30. Hanson DR, Lovejoy ER. Measurement of the thermodynamics of the hydrated dimer and trimer of sulfuric acid. J Phys Chem A. 2006;110(31):9525-8.

S31. Zhao J, Eisele FL, Titcombe, M., Kuang, C., McMurry PH Chemical ionization mass spectrometric measurements of atmospheric neutral clusters using the cluster-CIMS, J. Geophys Res,. 2010; 115, D08205.

S32. Jen C, Hanson DR, McMurry PH. Stabilization of the H2SO4 dimer by amines, submitted to J. Geophys. Res., 2014.

S33. Glasoe WA, Panta B, Volz K, Hanson DR et al.: Sulfuric acid: A systematic study of amines and experimental nucleation rates, in preparation, 2014.

S34. Clegg SL, Brimblecombe P. Solubility of ammonia in pure aqueous and multicomponent solutions. J Phys Chem. 1989;93(20):7237-48.

S35. Hanson D., and E. Kosciuch, J. Phys. Chem., 107, 2199-2108, 2003.

S36. Onel, L., Thonger, L., Blitz, M.A., Seakins, P. W., Bunkan, A. J. C., Solimannejad, M., and C. J. Nielsen, Gas-Phase Reactions of OH with Methyl Amines in the Presence or Absence of Molecular Oxygen. An Experimental and Theoretical Study, J. Phys. Chem. A, 2013, 117, 10736−10745.

Notes

Note 1. The pressure sensor for the source flow was found to lead to ions at masses 124 and 152 u and also probably 107 u. During the OK field mission, their signal intensity was variable but in general trended upward. These signals persisted in Minneapolis and began to decrease once the pressure sensor was removed and replaced with caps. These pressure sensors have a gel protecting the sensor which is the likely source of the contamination.

Note 2. The gas entering the vacuum system comprises about 80-120 sccm which would normally be supplied by clean cylinder gas. However, the recirculating zeroing procedure adopted here leads to a changing RH during a zero if a dry curtain gas is used. Since background signals are sensitive to RH, the curtain gas was eliminated. The recirculating zeroed air does not account for the flow into the vacuum thus the clean air also entrains about 6-to-10 % raw sample air. Therefore, a small bias may be introduced in the compounds that AmPMS monitors. A separate catalytic converter to supply curtain and source gases is planned for future missions.

Acknowledgment. This work was carried out in part (SI 6) using computing resources at the University of Minnesota Supercomputing Institute.